Autocrine VEGF–VEGFR2–Neuropilin-1 signaling promotes glioma stem-like cell viability and tumor growth

Petra Hamerlik,[1,2,3] Justin D. Lathia,[4] Rikke Rasmussen,[1] Qiulian Wu,[4] Jirina Bartkova,[1] MyungHee Lee,[1] Pavel Moudry,[5] Jiri Bartek Jr.,[6,7] Walter Fischer,[6] Jiri Lukas,[1] Jeremy N. Rich,[4] and Jiri Bartek[1,3,5]

[1]Danish Cancer Society Research Center and Centre for Genotoxic Stress Research, DK-2100 Copenhagen, Denmark
[2]Department of Clinical and Molecular Pathology, Faculty of Medicine and Dentistry, Palacky University, CZ-775 15 Olomouc, Czech Republic
[3]Institute of Molecular and Translational Medicine, Palacky University, CZ-775 15 Olomouc, Czech Republic
[4]Department of Stem Cell and Regenerative Medicine, Cleveland Clinic, Cleveland, OH 44195
[5]Department of Genome Integrity, Institute of Molecular Genetics, Czech Academy of Science, CZ-142 20 Prague 4, Czech Republic
[6]Department of Neurosurgery, Rigshospitalet, Blegdamsvej 9, DK-2100 Copenhagen, Denmark
[7]Department of Neurosurgery, Karolinska University Hospital, SE-141 86 Stockholm, Sweden

Although vascular endothelial growth factor (VEGF) receptor 2 (VEGFR2) is traditionally regarded as an endothelial cell protein, evidence suggests that VEGFRs may be expressed by cancer cells. Glioblastoma multiforme (GBM) is a lethal cancer characterized by florid vascularization and aberrantly elevated VEGF. Antiangiogenic therapy with the humanized VEGF antibody bevacizumab reduces GBM tumor growth; however, the clinical benefits are transient and invariably followed by tumor recurrence. In this study, we show that VEGFR2 is preferentially expressed on the cell surface of the CD133$^+$ human glioma stem-like cells (GSCs), whose viability, self-renewal, and tumorigenicity rely, at least in part, on signaling through the VEGF–VEGFR2–Neuropilin-1 (NRP1) axis. We find that the limited impact of bevacizumab-mediated VEGF blockage may reflect ongoing autocrine signaling through VEGF–VEGFR2–NRP1, which is associated with VEGFR2–NRP1 recycling and a pool of active VEGFR2 within a cytosolic compartment of a subset of human GBM cells. Whereas bevacizumab failed to inhibit prosurvival effects of VEGFR2-mediated signaling, GSC viability under unperturbed or radiation-evoked stress conditions was attenuated by direct inhibition of VEGFR2 tyrosine kinase activity and/or shRNA-mediated knockdown of VEGFR2 or NRP1. We propose that direct inhibition of VEGFR2 kinase may block the highly dynamic VEGF–VEGFR2–NRP1 pathway and inspire a GBM treatment strategy to complement the currently prevalent ligand neutralization approach.

CORRESPONDENCE
J. Bartek:
jb@cancer.dk
OR
J.N. Rich:
richj@ccf.org

Abbreviations used: CSC, cancer stem-like cell; EEA1, early endosomal antigen 1; GBM, glioblastoma multiforme; GSC, glioma stem-like cell; IR, ionizing radiation; NRP1, Neuropilin-1; VEGF, vascular endothelial growth factor.

GBM, the most prevalent primary malignant brain tumor in adults, is essentially universally fatal, despite maximal therapy. Robust neoangiogenesis and intratumoral heterogeneity are hallmark features of these brain malignancies, which contribute to their phenotypic plasticity and therapeutic resistance (Shen et al., 2008; Li et al., 2009a; Ricci-Vitiani et al., 2010; Wang et al., 2010; Soda et al., 2011). The latter includes drugs that target the angiogenic interplay between vascular endothelial growth factor (VEGF) and its receptors, VEGFRs. Recent observations suggest that anti-VEGF compounds (blocking antibodies and tyrosine kinase inhibitors), administered in combination with or before radiation, improve the responsiveness of solid tumors through radiosensitizing effects (Winkler et al., 2004; Citrin et al., 2006; Folkins et al., 2007; Vredenburgh et al., 2007; Desjardins et al., 2008; Ellis and Hicklin, 2008; Friedman et al., 2009; Gururangan et al., 2010; Lai et al., 2011).

The concept of cancer stem-like cells (CSCs) in general, and their presence in glioblastoma

The Rockefeller University Press $30.00
J. Exp. Med. Vol. 209 No. 3 507-520
www.jem.org/cgi/doi/10.1084/jem.20111424

multiforme (GBM) in particular, have been established, and markers to prospectively isolate these putative CSCs, such as the transmembrane glycoprotein CD133 (prominin-1), have been identified (Hemmati et al., 2003; Singh et al., 2003; Li et al., 2009b). However, the value of CD133 as a single marker of glioma stem-like cell (GSC) is controversial (Wu and Wu, 2009), as $CD133^-$ glioma cells can also give rise to tumors in an intracranial mouse model (Beier et al., 2007; Joo et al., 2008; Wang et al., 2008).

VEGFR2 (also known as kinase domain region or fetal liver kinase-1) is a tyrosine kinase receptor essential for VEGF-mediated physiological responses in endothelial cells (Shibuya, 2008). Traditionally, the VEGFRs were thought to be almost exclusively expressed by endothelial cells (Norden et al., 2009; Iwamoto and Fine, 2010). Recent studies, however, suggest that tumor-derived VEGF provides not only paracrine survival cues for endothelial cells, but may also fuel autocrine processes in GBM cells (tumor-secreted VEGF providing prosurvival signaling through VEGFRs expressed by tumor cells themselves) and play a role in tumor resistance to existing therapies (Gorski et al., 1999; Graeven et al., 1999; Knizetova et al., 2008; Hlobilkova et al., 2009). Moreover, a new phenomenon of GSCs' differentiation into tumor endothelium has been described and proposed to contribute to tumor neoangiogenesis and possibly to tumor resistance to antiangiogenic drugs (Shen et al., 2008; Ricci-Vitiani et al., 2010; Tokuyama et al., 2010; Wang et al., 2010; Soda et al., 2011).

In our present study, the VEGFR2 receptor was detected preferentially on the surface of $CD133^+$ GSCs when compared with their $CD133^-$ counterparts, and VEGF-VEGFR2 signaling promoted their viability and tumorigenic potential. Interestingly, we observed that VEGFR2 is not only presented on the cell surface of GSCs, but the bulk of the receptor is cytosolic, internalized at least in part in early endosomal compartment, while persisting in its autophosphorylated, active state. Furthermore, we found that NRP1, another important proangiogenic factor (Soker et al., 2002), interacts with and stabilizes VEGFR2 in the presence of VEGF ligand, and thus promotes VEGF-VEGFR2 pro-survival signaling.

To date, the cellular mechanisms that underlie the clinical response, including resistance to anti-VEGF and radiation therapy, are poorly understood. Mechanistically, the at least partially autocrine activation of the VEGFR2 receptor tyrosine kinase in GSCs suggests that successful therapeutic inhibition of VEGFR2 activity and/or its interaction with NRP1 might negatively impact $VEGFR2^+$ tumor cell growth and cause tumor regression.

RESULTS

Surface VEGFR2 is enriched in a fraction of GSCs in human GBM

Given the reported enhanced secretion of VEGF ligand by the CD133-enriched tumor cell population (Bao et al., 2006b; Folkins et al., 2009) and autocrine growth factor signaling contributing to tumor growth (Tokuyama et al., 2010), we hypothesized that there was a potential autocrine signal transduction through VEGFR2 in GSCs. We first performed quantitative flow cytometry analyses (FACS) of 17 freshly dissociated human GBM specimens (which were allowed to recover overnight in bFGF/EGF-supplemented neurobasal medium), and found enrichment of the surface VEGFR2 expression among $CD133^+$ cells compared with their $CD133^-$ counterparts (mean positivity 19.6% for $CD133^+$ versus 4.7% for $CD133^-$ cells; **, $P < 0.0017$; Fig. 1 A). The fraction of tumor cells positive for surface VEGFR2 varied among the tumor samples analyzed, ranging from 1.4 to 25.9% (mean $13.8 \pm 8.3\%$). To exclude that the $VEGFR2^+$ cells are tumor-associated endothelial cells, the following gating strategy was used in our experiments: dead cells were excluded by labeling with 7AAD, and then viable cells were gated as $CD133^+$ and $CD133^-$ subpopulations, each of which was depleted of cells expressing the endothelial marker CD31 (Newman et al., 1990). Potential contamination by other cell types was furthermore ruled out by flow cytometry analyses for CD144, CD31, CD34, and CD105 markers in the two GBM specimens (T556 and T1966) used throughout this study (Fig. S1). These analyses ensured that our experiments would be performed using a defined population of GBM cells, and revealed the existence of a subset of GBM cells expressing surface VEGFR2, particularly enriched among the $CD133^+$ tumor cells.

Interestingly, immunohistochemical analysis of paraffin-embedded clinical GBM specimens demonstrated that apart from the prominent membrane staining pattern of VEGFR2 seen in ~0.5–3% of GBM cells, the overall fraction of VEGFR2-expressing GBM cells was commonly higher, mainly showing a "punctate" cytosolic pattern of VEGFR2 (in 5–60% of GBM cells per lesion; Fig. 1 B). This finding inspired us to examine the ratio of surface versus cytosolic VEGFR2 fractions also by flow cytometry, since the cytosolic VEGFR2 may recycle back to plasma membrane and/or remain active in the cytosolic compartment, a phenomenon described in endothelial cells (Gampel et al., 2006; Ballmer-Hofer et al., 2011; Jopling et al., 2011). Indeed, FACS analysis could identify not only the surface (through surface labeling of viable cells), but also the cytosolic pool of VEGFR2 (visualized in the second labeling step after cell fixation/permeabilization, to detect total VEGFR2). Although the fraction of surface $VEGFR2^+$ cells (T12, 2.4%; T16, 5.5%; T18, 5.5%; T19, 17.4%) corresponded to those from FACS analysis presented above (Fig. 1 A), the number of total $VEGFR2^+$ cells was significantly higher (T12, 12.9%; T16, 11.8%, T18, 27.7%; T19, 44.4%), indicating presence of a cytosolic VEGFR2 pool (with cytosolic VEGFR2 in T12, 10.5%; T16, 6.3%; T18, 22%; T19, 27% cells; Fig. 1 C). Thus, whereas the presence of surface VEGFR2 "ready-to-bind VEGF" remains primarily the property of $CD133^+$ GSCs, the internalized VEGFR2 is detectable in a larger cell population within the tumor mass, likely available to be recycled to the cell surface. Such a dynamic behavior of VEGFR2 offers new possibilities for the putative communication of GSCs within their vascular niche,

through GSCs' ability to modulate this niche by self-controlled autocrine secretion of VEGF into cellular microenvironment.

To confirm that CD133$^+$ cells contain both, the surface-presented and cytosolic VEGFR2, we analyzed freshly dissociated xenografted specimens (T4121 and T3691) double-stained for surface VEGFR2/CD133, followed by fixation/permeabilization and additional staining for total VEGFR2 (see Materials and methods for details). As shown in Fig. 1 D, CD133$^+$ cells exhibit three patterns of VEGFR2: preferentially surface (T4121, 4.58%; T3691, 2.09%), surface and cytosolic (T4121, 12.3%; T3691, 10.7%), and cytosolic only (T4121, 27%; T3691, 40.5%). Consistent with our initial analyses, CD133$^-$ cells showed lower percentages of VEGFR2$^+$ cells for all three staining patterns. Furthermore, our immunofluorescence staining on frozen sections from human GBM biopsies confirmed the presence of a VEGFR2$^+$/CD133$^+$/CD31$^-$ cell population (Fig. 2 A) in close proximity to vascular structures.

Recently, the intimate interplay between the vascular and nervous system gained further support from studies on potential trans-differentiation (Ricci-Vitiani et al., 2010; Wang et al., 2010; Soda et al., 2011). In human brain, neural stem cells and endothelia localize to a vascular niche, where autocrine VEGF-mediated signaling is suggested to enhance viability of endothelial cells (Gorski et al., 1999). In this study, we commonly used GBM cells with surface expression of VEGFR2 (i.e., the subset that encompasses both the preferentially surface and surface + cytosolic VEGFR2, conveniently isolated by live-cell FACS sorting for surface VEGFR2), marked as VEGFR2^H cells. Orthotopically injected GFP-lentivirus–labeled VEGFR2^H/CD31$^-$ GBM cells contributed to tumor vessel formation in the mouse brain parenchyma as shown in Fig. 2 B, which is consistent with recent works (Ricci-Vitiani et al., 2010; Wang et al., 2010; Soda et al., 2011). When orthotopically implanted in immunocompromised mice, VEGFR2^H/CD31$^-$ cells formed tumors where VEGFR2 is persistently active in GBM cells, as assessed by immunofluorescence staining for Tyr1054-phosphorylated VEGFR2 on frozen sections from such xenografts (unpublished data).

These findings prompted us to examine whether and in which compartment VEGFR2 is active and what biological benefit could such autocrine VEGF-VEGFR2 signaling provide to GBM cells.

Autocrine VEGF-VEGFR2 signaling is enhanced by interaction with NRP1 and remains active in the endosomal compartment of GBM cells

Next, we asked whether Neuropilin-1 (NRP1), a nonsignaling co-receptor of VEGFR2 in endothelial cells (Ferrara et al., 2003), could be present in the GBM cells and possibly interact with VEGFR2 in our experiments. The endothelial NRP1

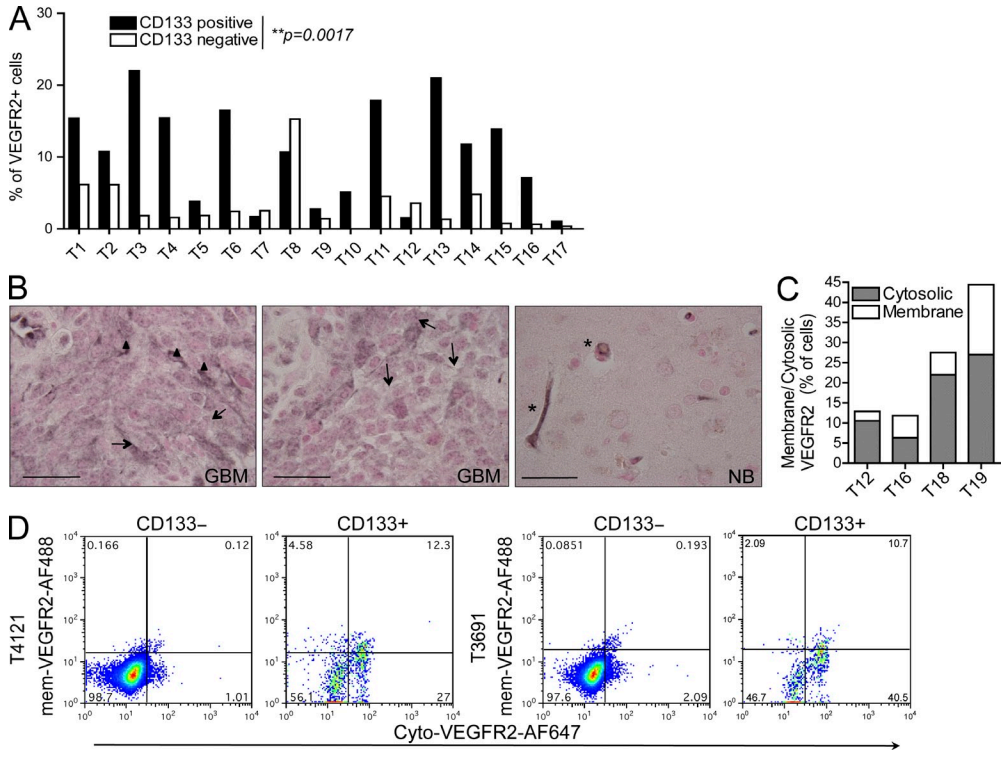

Figure 1. VEGFR2 is enriched on the surface of human GSCs. (A) Graph of cell surface VEGFR2$^+$ cell fractions among CD133$^+$ versus CD133$^-$ GBM cells based upon FACS analysis of 17 freshly dissociated human glioma specimens (**, P = 0.0017). (B) Immunohistochemical detection of VEGFR2 in clinical GBM specimens (left and middle image) of both surface (arrowhead) and intracellular (arrow; cytosolic) VEGFR2; normal brain (NB; right) shows VEGFR2 in endothelial cells/vessels (*). Bar, 50 µm. (C) Graph of surface and cytosolic VEGFR2 in 4 GBM (two independent experiments). (D) Representative plots of FACS-analyzed surface (mem) versus cytosolic (cyto) VEGFR2 in CD133$^+$ and CD133$^-$ GBM cells (specimens T4121 and T3691).

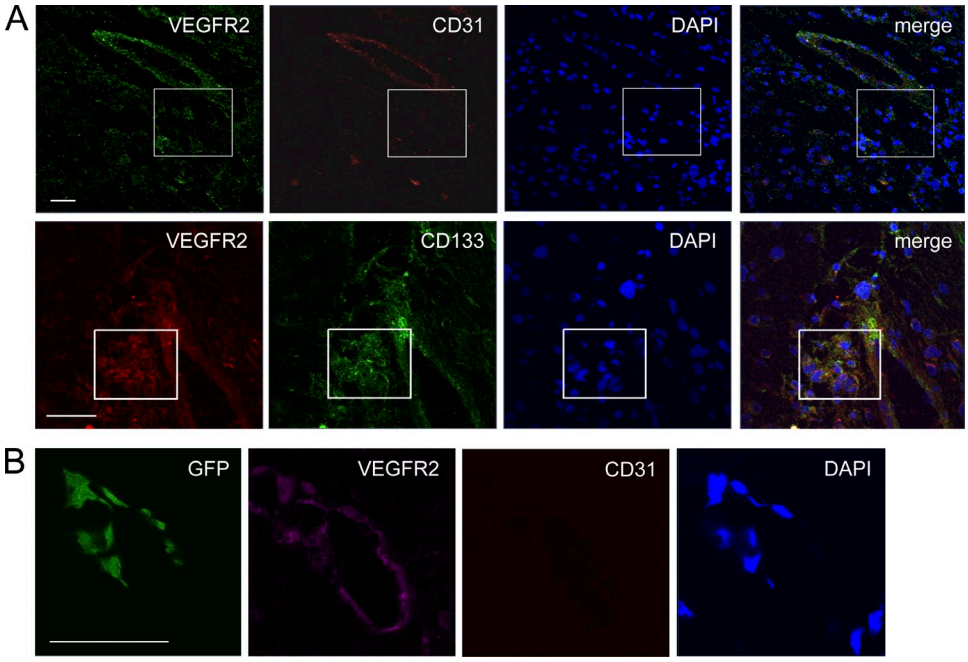

Figure 2. VEGFR2^{H} GBM cells localize in the perivascular niche in vivo. (A) Immunofluorescence on frozen sections of human GBM detects VEGFR2^{H}/CD133^{+}CD31^{-} cells next to tumor vessel. (B) Immunofluorescence on sections of human GFP-marked GBM VEGFR2^{H}/CD31^{-} (T556) cell xenografts after 15 d of tumor growth in mouse brain. Bars, 50 µm.

reportedly enhances VEGFR2–VEGF interaction, but only binds the $VEGF_{165}$ isoform, and thereby promotes pathological angiogenesis. Furthermore, overexpression of NRP1 in brain tumors correlates with disease progression (Ishida et al., 2000; Mac Gabhann and Popel, 2006; Hu et al., 2007; Pan et al., 2007; Jarvis et al., 2010), and therefore NRP1 represents a potential target for inhibiting VEGF signaling. Interestingly, NRP1 colocalized with autophosphorylated and total VEGFR2 in immunofluorescence on frozen sections from clinical GBM specimens (Fig. 3 A).

To further examine a potential role of NRP1 in VEGF–VEGFR2 signaling in GSCs, we compared coimmunoprecipitation of VEGFR2 and NRP1 in extracts from GBM cells that were untreated, treated with $VEGF_{165}$, pretreated with VEGFR2 tyrosine kinase inhibitor SU1498 followed by $VEGF_{165}$ treatment (100 µg/ml, 15 min), or treated by bevacizumab only (humanized antibody against VEGF). As shown in Fig. 3 B,VEGFR2 interacts with NRP1 in a ligand-dependent manner, as neutralization of VEGF by bevacizumab blocked formation of the VEGFR2–NRP1 complex. In contrast, inactivation of the tyrosine kinase activity by SU1498 had no significant effect on the VEGFR2–NRP1 interaction. $VEGF_{165}$ treatment further enhanced the basal level of activatory autophosphorylation at VEGFR2 Tyr1054. Pretreatment with bevacizumab abolished the basal level of VEGFR2 autophosphorylation, and treatment with SU1498 not only prevented the $VEGF_{165}$-induced increase, but even inhibited the activatory phosphorylation of VEGFR2 to a level below that seen under basal conditions (Fig. 3 B). These results show that VEGFR2 signaling in GSCs is active and dependent on VEGF ligand, whose increased levels can further enhance the activatory VEGFR2 autophosphorylation, which is apparently potentiated by interaction with the NRP1 co-receptor. Overall, these findings support a concept of VEGFR2 engagement in an autocrine VEGF ligand-dependent loop operating in GBM.

Moreover, shRNA-mediated knockdown of NRP1 resulted in dramatically decreased VEGFR2 protein levels, indicating a crucial role of NRP1 in VEGFR2 protein stability (Fig. 3 C). The observed decrease in total VEGFR2 was also accompanied by lower surface VEGFR2 presentation on the original VEGFR2^{H} GBM cells (unpublished data) and their decreased viability.

For most other receptor tyrosine kinases like EGFR and PDGFR, the majority of unliganded receptor is localized at the cell surface in ligand-unstimulated cells (Roberts et al., 2001; Wherlock et al., 2004). Upon activation, ligand–receptor complexes are commonly internalized to activate signal mediators until the complex is either degraded or recycled. Here, cell surface biotinylation followed by immunoprecipitation of biotinylated surface protein fraction, compared with cytosolic proteins, showed that in a freshly dissociated population of unstimulated GBM cells, a large proportion of the total VEGFR2 and active Tyr1054-phosphorylated VEGFR2 is localized in the cytosol (Fig. 3 D).

Furthermore, we found only a limited amount of VEGFR2 protein associated with the isolated biotin-labeled membrane fraction, which is consistent with known rapid internalization of VEGFR2 upon its activation (Lampugnani et al., 2006). Importantly, the same subcellular distribution profile was

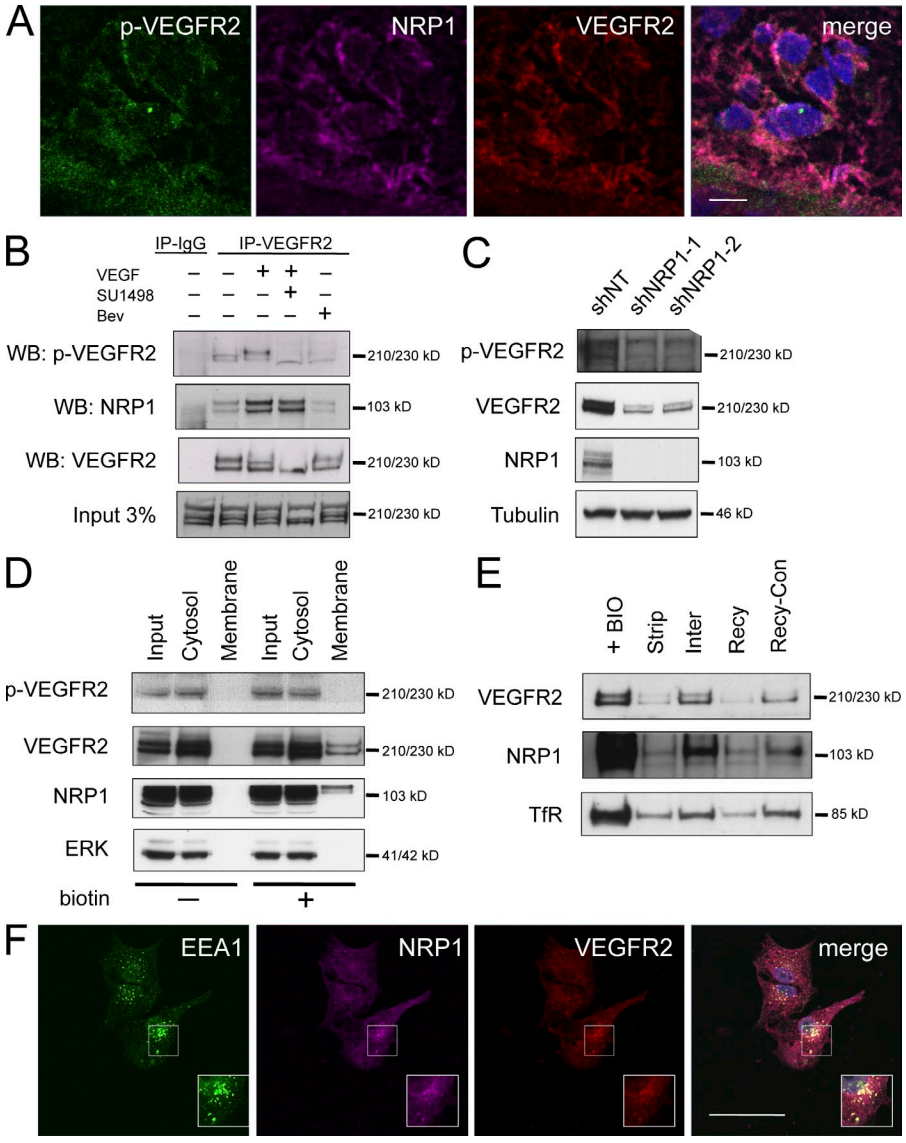

Figure 3. Total and activated VEGFR2 localize to the cytosol of GBM cells and undergo endocytosis and recycling. (A) Indirect immunofluorescence staining for VEGFR2, phosphorylated VEGFR2, and NRP1 on frozen sections of human gliomas. DAPI shown in blue. (B) Immunoprecipitation (IP)/Western blotting (WB) of VEGFR2 and NRP1 in GBM cells, lysed after overnight recovery/starvation of freshly dissociated specimen T556, pretreated or not with SU1498 (10 µM) or bevacizumab (Bev; 0.5 mg/ml) for 2 h, and then exposed (15 min) or not to recombinant $VEGF_{165}$ (100 µg/ml). pVEGFR2, Tyr1054-phosphorylated VEGFR2. Data are representative of three independent experiments. (C) Effect of shRNA knock-down of NRP1 in T556 GSCs on phosphorylated and total VEGFR2. Data are representative of two independent experiments. (D) Analysis of VEGFR, pVEGFR2 and NRP1 in membrane (biotin-labeled) and cytosolic (biotin-free) fractions of GBM T556 cells. ERK kinase: control cytosolic protein. Representative example from three experiments. (E) VEGFR2, NRP1, and TfR (positive control) examined during endocytosis and recycling. Biotinylated surface proteins (+BIO, high level); biotin label stripped immediately (Strip); proteins allowed to internalize for 10 min (Inter, partly protected from strip) and recycle for 20 min (Recy, de-protected by resurfacing again) before stripping, respectively. Recy-Con was performed along with Recy-sample, but the final stripping was omitted. Experiment is representative of three. (F) Confocal microscopy imaging in sorted $CD133^+$ GBM cells stained for VEGFR2, NRP1, and EEA1 (a marker of early endosomes). DAPI is shown in blue. Representative images of three independent staining experiments are shown. Bars: (A and F) 50 µm.

observed for NRP1, supportive of the role of NRP1 in VEGFR2 stability and signaling. Similarly, membrane fractionation showed the bulk of VEGFR2 to be present in the cytosolic pool, and at least partly active (unpublished data).

Importantly, experiments with cell surface protein biotinylation, followed by stripping of the surface-exposed biotin at various time points, confirmed recycling of VEGFR2, activated VEGFR2, and NRP1 (Fig. 3 E). Thus, the initially biotin-labeled membrane VEGFR2 and NRP1 (and transferrin receptor, a prototypic recycling receptor) were lost when surface-accessible biotin was stripped immediately, but protected from stripping when cells were allowed to internalize a fraction of their surface proteins for 10 min at 37°C (lanes +BIO, Strip, and Intern in Fig. 3 E, respectively) before the reducing strip. The observation that the second round of surface biotin stripping performed upon longer incubation time (after another 20 min at 37°C) apparently de-protected the transiently internalized, shielded fraction of VEGFR2 and NRP1 (Fig. 3 E, lanes Recy-con and Recy), is consistent with a surface-cytosol-surface recycling of VEGFR2–NRP1. Finally, immunofluorescence staining and confocal microscopy imaging confirmed colocalization of the cytosolic pool of VEGFR2–NRP1 with the early/recycling endosomal compartment marked by staining for early endosomal antigen 1 (EAA1; Fig. 3 F).

The plasma membrane complex of VEGFR2 with NRP1 is undergoing dynamic recycling from cell surface, through endosomal-internalized compartment back to cell membrane in human GSCs, and appears to be in an active state likely caused by persistent autocrine signaling from VEGFR2–NRP1 fueled by secreted VEGF.

Surface VEGFR2 enhances self-renewal capacity and viability of GSCs

Preferential deposition of VEGFR2 on the cell surface may be beneficial to GSCs' survival and propagation, as surface VEGFR2 is "ready to bind" VEGF produced by endothelial

or cancer cells present within the tumor microenvironment, followed by internalization and downstream signaling. One important prediction of such a concept would be that VEGFR2^{H} cells should exhibit higher capacity of self-renewal and superior growth in vitro and in vivo when compared with VEGFR2^{L} cell populations (i.e., GBM cells lacking both surface and cytosolic VEGFR2; see Materials and methods). To examine this, we sorted the VEGFR2^{H} and VEGFR2^{L} cells by FACS and assessed their tumor sphere formation capacity, a common surrogate assay of self-renewal. The results showed that the VEGFR2^{H} cells had a higher self-renewing potential than VEGFR2^{L} cells (Fig. 4 A; $P < 0.001$ for both T556 and T1966), which correlated with parallel viability tests performed on these sorted populations (Fig. 4 B) under identical cell culture conditions (in EGF/bFGF free medium to avoid VEGFR2 induction [Xiao et al., 2007] over a period of 7 d). These results indicate that the presence of VEGFR2 identifies GBM cells with enhanced propensity to proliferate and form spheres. Interestingly, when isolated and cultured in vitro for 5 d in growth factor–supplemented media, the VEGFR2^{L} cells exhibited enrichment and the VEGFR2^{H} cells further increase of surface VEGFR2 (unpublished data).

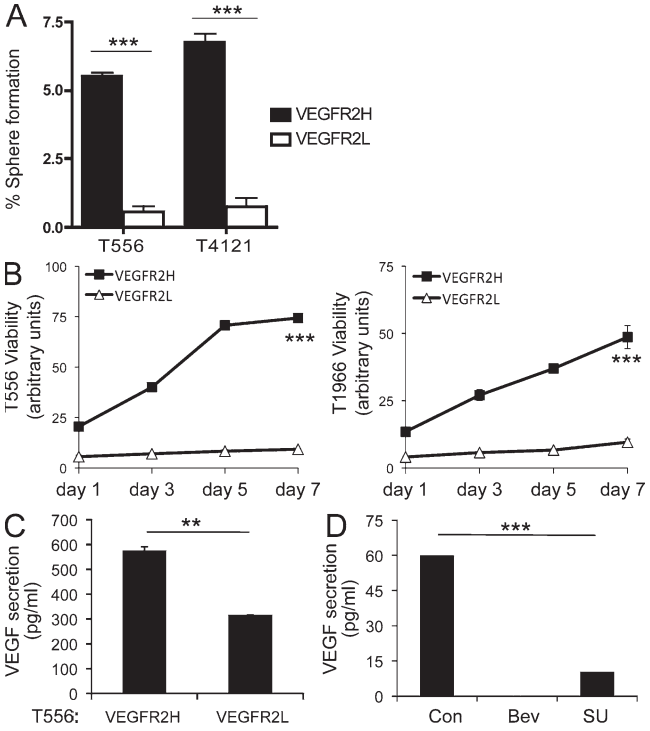

Figure 4. VEGFR2 expression accounts for enhanced self-renewal, VEGF secretion, and viability of GSCs. Matched numbers of VEGFR2^{L} and VEGFR2^{H} cells from xenografted GBM specimens (T556 and T4121) were assayed for tumorsphere formation (A) and (T556 and T1966) viability (B). (A) Data are means ± SD of two independent experiments ($n = 3$; $P < 0.001$). (B) Viability of GSCs. Data are means ± SD of two independent experiments ($n = 3$; $P < 0.001$). (C) VEGF secretion by VEGFR2^{H} versus VEGFR2^{L} cells (GBM T556, 24 h) detected by ELISA (**, $P < 0.01$). (D) ELISA-detected VEGF secreted by VEGFR2^{H} GBM cells after neutralization by bevacizumab (0.5 mg/ml, 24 h), and inhibition of VEGFR2 kinase (SU1498, 5 µM), compared with nontreated controls (Con). Mean ± SD from two experiments in duplicate (***, $P < 0.001$).

To gain further insights into GSCs' VEGFR2 signaling, we assessed VEGF secretion by VEGFR2^{L} and VEGFR2^{H} cells. The two cell subsets were sorted from bulk tumor populations by FACS, and, after an overnight recovery, allowed to secrete into growth factor–free media for 24 h. The VEGF levels of the resulting conditioned media were then analyzed using ELISA. As illustrated in Fig. 4 C, significantly elevated secretion of VEGF was detected for VEGFR2^{H} cells. To further explore the emerging autocrine activation of VEGFR2, VEGFR2^{H} GBM cells were treated with bevacizumab (known to block VEGF), SU1498 (VEGFR2 tyrosine kinase inhibitor), or vehicle control for 24 h, followed by detection of secreted VEGF by ELISA. In contrast to control, no secreted VEGF was detected in the medium of bevacizumab-treated cells, showing efficient VEGF ligand neutralization by bevacizumab, as expected (Fig. 4 D). VEGF secretion was significantly decreased in SU1498-treated VEGFR2^{H} cells.

As the most crucial property of GSCs is their ability to propagate secondary tumors, we also performed in vivo limiting dilution assays using cells enriched for VEGFR2 (VEGFR2^{H}) compared with VEGFR2^{L} cells, independent of other markers. Although both types of cells formed tumors upon transplantation in vivo, there was a consistent trend for VEGFR2^{H} to develop tumors with a shorter latency. Notably, the superior tumorigenicity of VEGFR2^{H} cells was most apparent at the lowest number of GBM cells implanted (100 cells per mouse), which showed statistically significant differences, as documented by the Kaplan-Meier survival analysis (Fig. 5 A; $P = 0.0067$). However, differences in the experiments with 1,000, 5,000, or 10,000 cells injected per mouse did not reach statistical significance with respect to the VEGFR2 expression status (for information on tumor incidence and median survival see Table S1). As others and we have shown that the microenvironment can induce plasticity of cellular differentiation, we argued that one possible explanation for these results could be if the initial VEGFR2^{L} GBM cells reexpressed VEGFR2 during the in vivo growth. This scenario was indeed confirmed in vitro, as treatment of initial VEGFR2^{L} cells with the proteasomal inhibitor MG132 resulted in relatively fast (within 10 min) stabilization of VEGFR2 protein in these cells (unpublished data), indicating rapid turnover and sensitive modulation of VEGFR2 at the protein level.

Collectively, these results raise the issue of what are the functional consequences of the observed enhanced expression of VEGFR2 and the basis of its potential downstream signaling in this cellular context. Furthermore, we speculated that the observed persistent activation of VEGFR2 signaling in human GBM cells, along with the functionality of the VEGF–VEGFR2–NRP1 pathway but without any major biological impact of exogenously added VEGF (unpublished data), might reflect an ongoing autocrine loop between the secreted VEGF and VEGFR2 in the VEGFR2^{H} subset of GSCs.

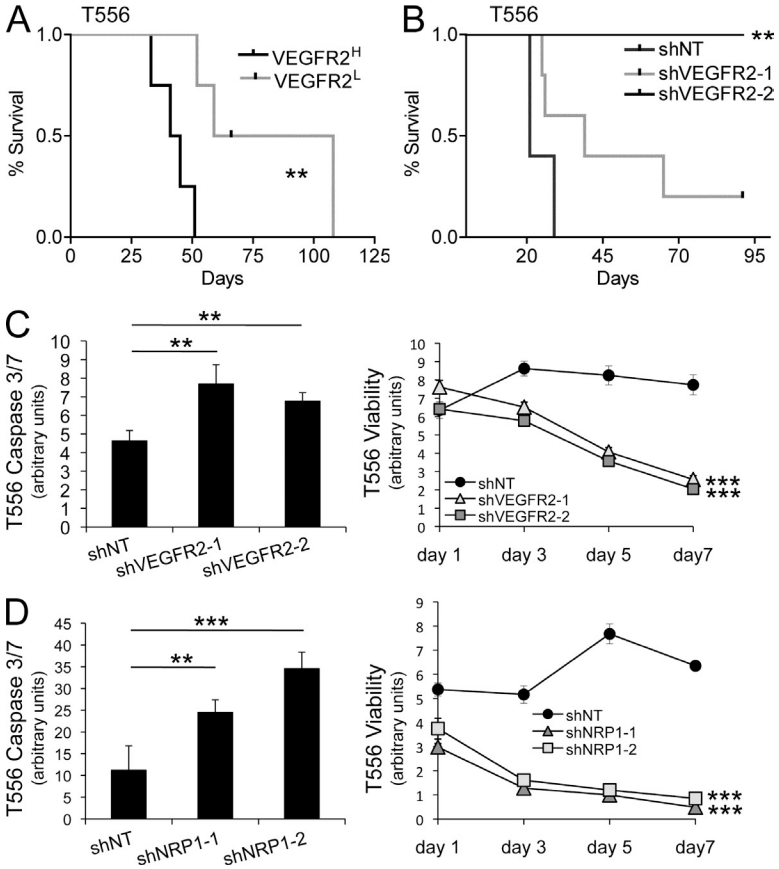

Figure 5. VEGFR2–NRP1 expression in GSCs accounts for preferential growth and survival in vitro and in vivo. (A) Kaplan-Meier survival curves for mice brain transplanted with VEGFR2^{H} versus VEGFR2^{L} human T556 GBM cells (4 mice per group; **, P = 0.0067, log-rank analysis). (B) Kaplan-Meier survival curves for mice after brain transplantation of T556 GSCs with lentivirus-mediated knockdown of VEGFR2 via two shRNAs (shVEGFR2-1 and shVEGFR2-2 targeting human VEGFR2), compared with a nontargeting shRNA (shNT). 5 mice per group; P = 0.0754 for shVEGFR2-1; **, P = 0.0054 for shVEGFR2-2 by log-rank analysis. (C) GSC death (T556; caspase 3/7 activity, left) and viability (right) after VEGFR2 knockdown (shVEGFR2-1 and shVEGFR2-2) compared with a nontargeting shRNA (shNT). $n = 3$; P = 0.0061 for shVEGFR2-1; P = 0.0024 for shVEGFR2-2 for caspase 3/7; P < 0.001 for shVEGFR2-1 and -2 for viability. (D) GSC death (T556; caspase 3/7 activity, left) and viability (right) after NRP1 knockdown (shNRP1-1 and shNRP1-2) compared with control shNT. $n = 3$; P = 0.0001 for both NRP1 shRNAs in either assay. (C and D) Data are means ± SD from three independent experiments.

Abrogation of VEGF–VEGFR2 signaling compromises GBM cell survival and tumorigenesis

To assess the contribution of VEGFR2 signaling to GSC self-renewal, survival, and tumor growth, we interrogated the effects of shRNA directed against human VEGFR2. VEGFR2^{H} GBM cells were infected with lentivirus particles expressing shRNA directed against VEGFR2 (shVEGFR2-1 and shVEGFR2-2 for targeting two independent gene regions) or a nontargeting control shRNA (shNT). After selection for successfully expressed vectors, cells for each of the three scenarios (shNT, shVEGFR2-1, and shVEGFR2-2) were analyzed in vitro (for viability and levels of apoptosis), and then implanted into the brains of immunocompromised mice.

As shown in Fig. 5 (B and C), shRNA-mediated knockdown of VEGFR2 resulted in increased apoptosis (measured by caspase 3/7 activity) and decreased viability of the shRNA-treated VEGFR2^{H} cells. Consistent with in vitro data, tumors in mice implanted with VEGFR2^{H} cells carrying the control shNT grew with expected, rapid kinetics, whereas shRNA-mediated knockdown of VEGFR2 resulted in reduced tumor formation and prolonged survival of the mice. Notably, compared with the control mice, which had to be sacrificed because of gross tumor growth before day 30 of the experiment, mice in the shVEGFR2-2 group were all still alive and free from major signs at day 90, and the shVEGFR2-1–treated group showed an intermediate phenotype (caused by cells escaping lentivirus-mediated shRNA knockdown and thus allowing for re-expression of VEGFR2, as confirmed by indirect immunohistochemistry staining on sections from paraffin-embedded brains from these mice; unpublished data). These genetic experiments are important as they validate the significance of VEGFR2 for GBM cell survival and support data (see below) obtained after chemical inhibition of VEGFR2 kinase activity. Consistent with the evidence for an important role of NRP1 in this pathway (Figs. 3 and 4), shRNA-mediated knockdown of NRP1 resulted in enhanced apoptosis and decreased viability of GSCs, thus further supporting the role of VEGFR2–NRP1 interaction in GSCs' survival (Fig. 5 D).

To test whether the observed autocrine signaling through the VEGF–VEGFR2–NRP1 pathway might be critical for survival of the VEGFR2-expressing GBM cells under normal and stressful conditions, we treated the VEGFR2^{H} cells with the VEGFR2 kinase inhibitor SU1498 (5 μM, 2 h) alone or in combination with ionizing radiation (IR) to mimic the genotoxic stress caused by radiotherapy. As shown in Fig. 6 A, inhibition of VEGFR2 tyrosine kinase activity in VEGFR2^{H} GBM cells induced apoptosis as indicated by increase in Annexin V staining monitored by flow cytometry at 24 h after radiation. The enhanced cell death after treatment with SU1498 was apparent under otherwise unperturbed culture conditions, and this effect was further enhanced when cells were stressed by IR. In contrast to inhibition of VEGFR2 kinase activity, treatment with the VEGF-blocking antibody bevacizumab alone did not significantly increase apoptosis (Lai et al., 2011). These results highlight the differential impact of the biologically effective direct inhibition of VEGFR2 tyrosine kinase activity (by SU1948) versus the apparent inability of bevacizumab to evoke a desirable antitumor effect. We speculate that the latter phenomenon might reflect insufficient neutralization by bevacizumab of the continuously

secreted VEGF ligand, thereby allowing for VEGFR2 signaling and, consequently, continued survival and growth of the tumor.

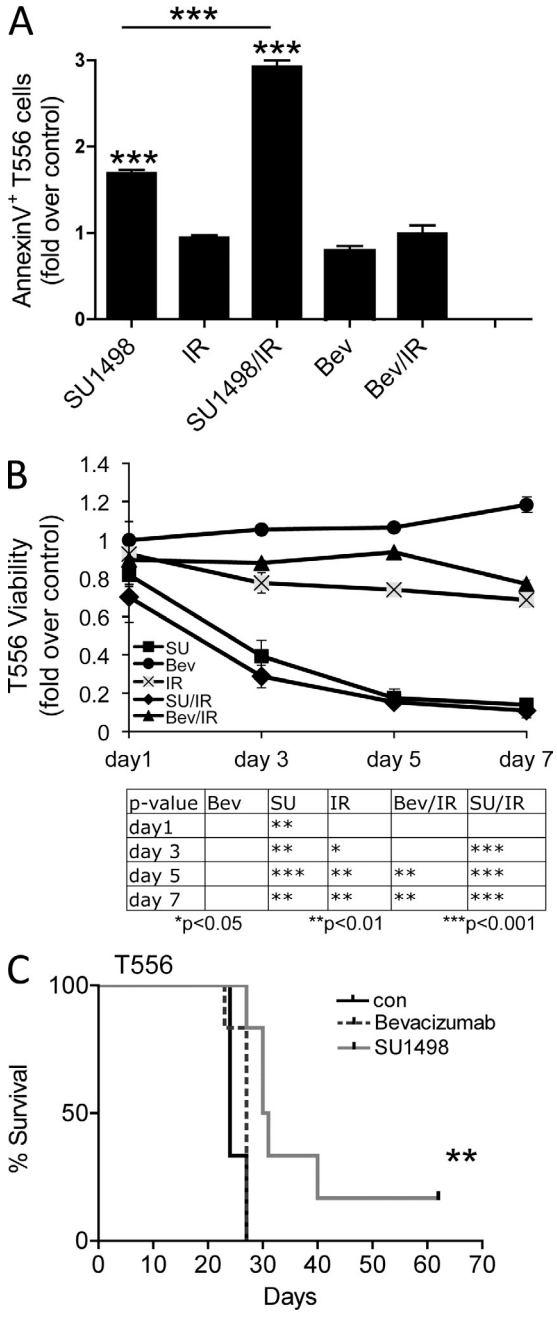

Figure 6. Chemical abrogation of VEGFR2 signaling decreases survival and enhances apoptosis in T556 GSCs. (A) Annexin V FACS analysis of dissociated xenograft VEGFR2^{H} cells pretreated with bevacizumab (Bev, 0.5 mg/ml) or SU1498 (SU, 5 µM) or untreated for 2 h, and then irradiated (IR, 8 Gy) or sham-irradiated, and stained 24 h after IR for Annexin V. Mean ± SD (n = 3); one of two experiments with similar results. (B) Effect of SU1498 or bevacizumab alone or combined with IR on cell growth of VEGFR2^{H} cells (P = 0.0047). Mean ± SD (n = 3). Representative of three experiments is shown. (C) Survival effect of in vitro pretreatment of VEGFR2^{H} cells with SU1498 (10 µM; 24 h) or bevacizumab (0.5 mg/ml; 4 d) on their tumorigenicity in vivo (n = 6; **, P = 0.0078 by log-rank analysis of survival curves).

To corroborate the emerging differential biological impact of VEGFR2 kinase inhibition versus VEGF ligand neutralization, VEGFR2^{H} cells were treated with either SU1498 or bevacizumab or left untreated, irradiated, or sham-irradiated, and then followed for 7 d to assess their relative cell viability (measured by the CellTiter-Glo kit; Fig. 6 B). Although bevacizumab treatment alone did not impact the viability of VEGFR2^{H} cells, exposure to 5 µM SU1498 led to a significant decrease in cell viability, and this effect was further increased when inhibitor treatment was followed by IR. In agreement with published results (Iwamoto et al., 2009), bevacizumab in combination with IR also resulted in a significant decrease in cell viability, but this effect was less pronounced compared with tyrosine kinase inhibition by SU1498. These results were reproduced in a series of experiments with independent specimens, T556 (Fig. 6) and T1966 (unpublished data). To determine if these results are reproducible in vivo, we pretreated VEGFR2^{H} cells in vitro with bevacizumab (for 4 d), VEGFR2 tyrosine kinase inhibitor SU1498 (24 h), or left untreated and injected 10^4 cells into frontal lobes of immunocompromised mice. Fig. 6 C shows that targeting the VEGFR2 tyrosine kinase activity, but not ligand neutralization, is sufficient to impair tumor propagation.

Collectively, these results supported our concept that persistent autocrine VEGFR2 signaling represents a potent regulator of GSC growth under both in vitro and in vivo conditions. Moreover, this signaling apparently not only operates in GSC cell pools, but stays active in a larger pool of progeny tumor cells, which can reactivate the autocrine loop by recycling internalized VEGFR2 back to the cell surface. In conclusion, the functional abrogation of the VEGFR2–NRP1–VEGF–regulated pathways can undermine GBM survival under various conditions, including exposure to IR, and reduce tumor formation.

DISCUSSION

Our present results provide novel insights into the molecular basis of the emerging interplay between GSCs and tumor angiogenesis, the ensuing strengths and vulnerabilities of GSCs, and the implications of the identified VEGFR2-mediated signaling loop for gliomagenesis and response to therapy. As angiogenesis and CSCs are important for other types of cancer as well (Reya et al., 2001; Eyler and Rich, 2008), our findings may help advance understanding of cancer biology in general, and provide valuable clues for future therapeutic strategies, as gliomas remain a major therapeutic challenge (Norden and Wen, 2006; Rich, 2007; Verhoeff et al., 2009). The concept emerging from our study can be summarized as follows: GSCs rely on an autocrine, highly dynamic signaling pathway that involve (a) VEGF and its secretion; (b) VEGFR2 and its interaction with NRP1; and (c) dynamic VEGFR2–NRP1 internalization/recycling, to survive, proliferate, form tumors (including crosstalk with vascular niche), and evade some forms of currently used therapy. Several elements of this concept are discussed in the following paragraph, within the framework of recent developments in cancer research.

First, the search for convenient molecular markers and critical functional features of CSCs has been a focus of cancer research for almost a decade. Because of the highly heterogeneous character of gliomas, it is difficult to use a single set of markers to identify CSCs in individual glioma patients. Despite major advances in this area, the candidate markers exemplified by CD133 for GSC enrichment have so far been insufficiently selective and/or remain enigmatic in terms of their functional significance and relevance for cancer therapy (Wu and Wu, 2009). As a consequence, the definitions of GSCs presently reflect the biological properties of these cells (Calabrese et al., 2007; Rich, 2007; Li et al., 2009b). In addition to CD133, other markers like A2B5 and CD15 have been identified (Ogden et al., 2008; Son et al., 2009). Because glioma cells expressing either only A2B5 or CD15 irrespective of their CD133 status formed tumors in rodent hosts, they appear to identify a new glioma CSC population. Other recently identified promising markers include podoplanin, a proinvasive protein overexpressed in a variety of cancers (Christensen et al., 2011), and integrin α6 (Lathia et al., 2010), which is known to play a crucial role in the maintenance of normal neural stem cells (Leone et al., 2005). We now report that the VEGFR2 receptor is enriched on the surface of GSCs and that the VEGFR2-mediated signaling pathway is active in an autocrine-produced VEGF ligand-dependent manner. Although we do not propose that VEGFR2 is a specific marker of GSCs, the expression of the surface VEGFR2 was indeed commonly enriched among the $CD133^+$ cells in a panel of the 17 GBM specimens tested. Central to this concept is the observation that a significant pool of VEGFR2 is contained within the cytosol and, based on microscopic analysis, localized predominantly in the early endosomal storage compartment. Besides being degraded, a subfraction of cytosolic VEGFR2 remains active and recycles back to the cell surface. Our present data (Fig. 3 E) on GBM, and studies by others in endothelial cells (Gampel et al., 2006; Jopling et al., 2011), have shown that VEGFR2 undergoes recycling from peripheral endosomes back to the plasma membrane, but the regulatory molecules involved remain unclear.

Our data not only corroborate that GSCs secrete VEGF to possibly stimulate endothelial cells and angiogenesis in a paracrine manner, as postulated before (Bao et al., 2006b; Folkins et al., 2009) but also show for the first time that GSCs harbor an operational VEGFR2-dependent autocrine signaling loop, capable of responding to VEGF and transducing downstream signaling. We show that this pathway also encompasses the VEGF-dependent interaction of VEGFR2 with NRP1, a high-affinity receptor for semaphorins and VEGF reported for cell types, such as neurons and endothelia (Ferrara et al., 2003; Rosenstein and Krum, 2004), but so far not for GSCs. Although NRP1 does not seem to induce intracellular signaling on its own, likely because of the lack of a cytoplasmic kinase domain, it is known to potentiate angiogenesis by facilitating the interaction between $VEGF_{165}$ and VEGFR2, resulting in increased VEGF–VEGFR2 signaling in endothelial cells (Soker et al., 2002). Apart from interaction with NRP1, we show that this GSC-associated VEGF–VEGFR2–NRP1 pathway is regulated at several steps, including autocrine secretion of VEGF (higher for the $VEGFR2^H$ cells), and regulation of VEGFR2 protein stability, as lentivirus-mediated knockdown of NRP1 resulted in significantly decreased VEGFR2 levels (Fig. 3 C) and dramatically decreased survival of GSCs caused by enhanced apoptosis (Fig. 5 D). Mac Gabhann and Popel (2006) predicted three alternative methods of targeting NRP1, resulting in three distinct therapeutic outcomes. Their in silico analysis has shown that the blockage of NRP1–VEGFR2 interaction is the most efficient way of attenuating VEGF–VEGFR2 signaling for a defined period of time. Their in silico findings, together with our in vitro evidence of NRP1 knockdown decreasing GSC viability, highlight the need for further identification of compounds targeting both VEGFR2 and NRP1 and the interactions between the two of them.

Considering the intimate relationship between GSCs and endothelium in the GBM perivascular niche (Gilbertson and Rich, 2007) and the prosurvival role of the VEGF–VEGFR2 pathway shared by both cell types, it is intriguing that the regulatory mechanisms we describe here for VEGFR2 protein in GSCs apparently differ markedly from that in vascular endothelium. The reported protein half-life of VEGFR2 in endothelial (HUVEC) cells was considerably longer (70 min) compared with 42 min in our experiments with GSCs (unpublished data). Even more striking, however, is the contrasting impact of proteasome inhibition on VEGFR2 protein abundance. Thus, for endothelial cells Meissner et al. (2009) reported that diverse proteasome inhibitors (including MG132) blocked VEGFR2 expression in a time- and concentration-dependent manner, and decreased VEGFR2 protein levels were paralleled by impaired formation of capillary-like structures and endothelial cell migration (Meissner et al., 2009). In sharp contrast, we observed that in $VEGFR2^L$ cell population, the VEGFR2 protein became stabilized and its levels increased already after a short-term exposure to the proteasome inhibitor MG132 (unpublished data). For endothelial cells under hypoxia, Kremer et al. (1997) suggested a direct transcriptional induction of VEGF that subsequently evoked up-regulation of VEGFR2. In neural stem cells, expression of VEGFR2 is up-regulated by bFGF-evoked signaling via phosphorylation of ERK1/2 (Xiao et al., 2007). We interpret these results as evidence for regulation of VEGFR2 in GSCs by rapid proteasome-mediated protein turnover, and indication that VEGFR2 is subject to highly flexible and prompt control that are broadly analogous to key regulators of the cell cycle and cell viability/death pathways (e.g., cyclins, NF-κB inhibitors, etc.).

The relevance of the VEGF–VEGFR2 pathway regulation becomes particularly apparent under stressful conditions such as tumorigenesis or exposure to IR, the latter representing the most commonly used standard-of-care nonsurgical treatment modality for GBM (Norden and Wen, 2006; Norden et al., 2009). During growth in cell culture within a relatively short time, a subset of originally $VEGFR2^L$ GBM cells became $VEGFR2^H$ (unpublished data). This adaptive change was mainly attributable to posttranscriptional regulation, as

VEGFR2 mRNA was also initially expressed in the VEGFR2^{L} cells (unpublished data). More importantly, given our evidence for the role of VEGFR2 signaling in the survival of GSCs, these findings may help explain why the initially VEGFR2^{L} GBM cells were only moderately less tumorigenic in vivo compared with their VEGFR2^{H} counterparts. Such an autoenhancing system, stabilizing/recycling VEGFR2 to plasma membrane and thereby becoming accessible to VEGF ligand, may represent an important mechanism contributing to tumor survival, angiogenesis, and progression after radiotherapy, likely linked to the debated greater resistance of GSCs, compared with the bulk of GBM cells, to radiation and chemotherapy (Bao et al., 2006a,b; Liu et al., 2006; Eyler et al., 2008).

Arguably the most significant data from our present study document the strikingly differential impact of the two strategies that are commonly used in the clinic to target the VEGF–VEGFR2 signaling cascade, i.e., the VEGF-blocking antibody bevacizumab versus chemical inhibition of VEGFR2 kinase activity. Given the characteristically high degree of endothelial proliferation, high vascular permeability, and increased proangiogenic growth factor expression, angiogenesis inhibition became a rational treatment strategy in GBM (Lai et al., 2011). However, despite some transient positive therapeutic impact of bevacizumab, the clinical trials of such VEGF-neutralizing strategies have been largely disappointing (Shintani et al., 2006; Desjardins et al., 2008; Friedman et al., 2009; Iwamoto et al., 2009; Gururangan et al., 2010; Verhoeff et al., 2010; Lai et al., 2011). Dynamic imaging methods revealed that antiangiogenic treatment is effective against the leaky bulk of the tumor, but not against invasive tumor components (Ellis and Hicklin, 2008), and an overall better understanding of angiogenesis and its molecular basis are needed to optimize the treatment. Our present results provide novel insights into this area of GBM research. Whereas most of current antiagiogenetic approaches act through the reduction or elimination of tumor blood vessels, we propose that dual targeting of not only the tumor vessels but also the tumor cells is important, as these operate typical endothelial prosurvival pathways like VEGF–VEGFR2–NRP1 signaling. We show that treatment of VEGFR2^{H} cells with tyrosine kinase inhibitor SU1498, but not with bevacizumab, resulted in enhanced apoptosis and decreased viability and tumorigenesis (Fig. 6 and not depicted). Notably, the results obtained with the VEGFR2 kinase inhibitor were reproduced using a genetic approach, by knocking down VEGFR2 through lentivirus-mediated shRNA (Figs. 5, B and C). In fact, the extent of the observed biological effects on survival and tumorigenicity correlated with the degree of VEGFR2 knockdown achieved by the two independent shRNAs, thereby further validating the superiority of direct targeting of VEGFR2 over sequestration of VEGF by bevacizumab. Taking into consideration our present data, as well as the available information on GSCs biology, angiogenesis, and response of GBM to antiangiogenic treatment, we propose a new model that may explain the differential impact of bevacizumab and VEGFR2 inhibition. We believe that not only the known paracrine function of VEGF from GSCs (Bao et al., 2006b; Folkins et al., 2007) but also the persistent autocrine signaling through the VEGF–VEGFR2 loop described here contributes to enhanced GBM cell survival in general, and tumorigenic properties and evasion of treatment by bevacizumab by GSCs in particular. Sakariassen et al. (2006) have shown that blocking angiogenesis using bevacizumab in an immunodeficient nude rat model results in angiogenic-independent GSC tumor growth with the up-regulation of proinvasive genes. In respect to recently published data on the existence of endoglial progenitors (Shen et al., 2008; Ricci-Vitiani et al., 2010; Wang et al., 2010; Soda et al., 2011) and our own data showing that VEGFR2^{H} cells contribute to vessel formation (Fig. 2 B), it is possible that after bevacizumab therapy, newly formed vessels (from endoglial precursors) substitute the original tumor vasculature, resulting in a subsequent diffuse relapse. The impact of bevacizumab might also be limited in the longer term, at least in part because of the continuous supply of VEGF newly secreted by GSCs themselves that immediately activates their own VEGFR2 receptors, thereby either saturating the binding capacity of bevacizumab or possibly bypassing the stage of a free extracellular VEGF ligand that is accessible by bevacizumab. Thus, combinational treatment including not only VEGF ligand neutralization but also efficient VEGFR2 tyrosine kinase activity inhibition may have improved activity. Whereas we observed a strikingly decreased viability of GBM cells after chemical or genetic abrogation of VEGFR2 tyrosine kinase activity, apparently conflicting results were reported from clinical trials in which agents targeting VEGFR2 tyrosine kinase domain were delivered in conjunction with chemotherapy and resulted only in a transient increase in patients survival, with majority of patients succumbing to tumor reocurrence (Butler et al., 2010; Hess et al., 2001). This might be an indication of insufficient targeting/inhibition of VEGFR2 tyrosine kinase, which we found to be internalized in a subpopulation of GBM cells. Thus, various combinations of strategies, including the development of novel potent tyrosine kinase inhibitors against VEGFR2 and possibly abrogating its interaction with NRP1, should be investigated (conveniently combined with radiotherapy or chemotherapy) to achieve synergistic effects on GSC apoptosis and so glioma regression.

In conclusion, the VEGF–VEGFR2–NRP1-mediated signaling in GSCs is maintained in an autocrine manner by continuous secretion of VEGF ligand, allowing for persistent activation of downstream intracellular prosurvival pathways and promotion of GBM tumor growth, invasiveness, and enhanced resistance to some treatments. This concept offers new insights into GBM biology and identifies the VEGF–VEGFR2–NRP1 interplay as a novel and attractive target in therapy of malignant gliomas.

MATERIALS AND METHODS

Human glioma xenografts and primary specimens. GBM tissue samples (T1-T19, T556, T1966, T4121, and T3691) were obtained from patients undergoing resection for newly diagnosed or recurrent tumors in

accordance with a protocol approved by the Central Scientific Ethics Committee of the Copenhagen University Hospital or the Cleveland Clinic Foundation Institutional Review Boards.

Tumor dissociation, cell culture, and FACS analysis and sorting. Tumors were dissected, washed in Earle's balanced salt solution, digested with papain (Worthington Biochemical), and filtered through 70-µm cell strainers to remove tissue pieces. Dissociated cells were then cultured overnight in Neurobasal A media supplemented with B27, epidermal growth factor, and basic fibroblast growth factor at 20 ng/ml (Invitrogen) before cell sorting, to allow for recovery of cell surface antigens. Freshly dissociated glioma specimens were labeled with conjugated antibodies (human-specific VEGFR2-Alexa Fluor 647 [BioLegend]; CD34-Alexa Fluor 488, CD105-Alexa Fluor 488, CD144-Alexa Fluor 488 [Miltenyi Biotec]; CD31-Alexa Fluor 488/CD31-PE [BioLegend]; and CD133/2-PE [Miltenyi Biotec]) and analyzed using the FACSCalibur (BD) cell cytometry analyzer, and acquired data were further processed using FlowJo software (Tree Star). Using a human-specific anti-VEGFR2 antibody allowed us to avoid any contamination by VEGFR2$^+$ mouse cells when dissociated xenotransplanted human GBM were analyzed. VEGFR2$^+$ (VEGFR2^H) and VEGFR2$^-$ (VEGFR2^L) cell fractions were sorted using MoFlo XDP Cell Sorter (Beckman Coulter), as follows: low expression (L), bottom 10% of GBM cells among the fraction, showing no surface VEGFR2 binding compared with isotype IgG-AF647 control (these were also validated as negative for cytosolic VEGFR2); high expression (H), GBM cells with a surface VEGFR2 signal above values of isotype IgG-AF647 control (typically around 5% of all GBM cells used in our study).

Immunofluorescence, microscopy, and Annexin V staining. Immunofluorescence staining for frozen glioma sections and xenografted GBM specimens for VEGFR2, VEGFR2Tyr1054, NRP1, CD31, EEA1, and CD133 was performed as described previously (Lathia et al., 2010). Examination was done using the LSM 510 META/Imager.Z1 (Plan-Apochromat 63×/1.40 oil DIC M27 objective; Carl Zeiss, Inc.). Confocal images were acquired with equal settings and processed with Zen 2008 software (Carl Zeiss, Inc.). For Annexin V staining, cells were labeled with Alexa Fluor 488–conjugated Annexin V for 15 min in Annexin V–binding buffer according to the manufacturer's instructions (Invitrogen). For analysis, the VEGFR2^H cell population was sub-gated and analyzed for the percentage of Annexin V–Alexa Flour 488–positive cells using FlowJo software.

Immunohistochemical analysis on paraffin sections. Formalin-fixed, paraffin-embedded specimens of human normal (n = 5) and GBM tumor (n = 15) brain tissues were examined, as follows. The tissue sections were deparaffinized and processed for sensitive immunoperoxidase staining with the primary antibody against human VEGFR2 (Cell Signaling Technology; diluted 1:250) incubated overnight, followed by detection using the VECTASTAIN Elite kit (Vector Laboratories) and nickel sulfate enhancement without nuclear counterstaining, as previously described (Bartkova et al., 2005). Alternatively, antibody-stained sections were counter-stained with either Fast Red or hematoxylin, using standard dyes and procedures, to better visualize cell morphology. Immunostaining on each slide was scored by an experienced pathologist, to examine the percentage of cell surface and intracellular pattern of VEGFR2 positivity in the tumor cells, as assessed in at least 400 GBM cells in 10 large, random microscopic fields per section.

Ionizing radiation and drug treatment. VEGFR2^H cells were left to recover overnight after sorting, and then pretreated with 5 µM (10 µM for IP experiment) VEGFR2 small molecule kinase inhibitor SU1498, 0.5 mg/ml bevacizumab, or left untreated for 2 h. Next, cells were sham-irradiated or exposed to ionizing radiation of 8 Gy that was delivered at the dose rate 2.18 Gy/min by an x-ray generator (Pantak; HF160; 150 kV; 15 mA). For MG132 (10 µM; EMD) treatment, cells were treated for indicated time points, and then subjected to Western blot analysis for VEGFR2 expression (see below). For in vivo tumor formation experiments, VEGFR2^H cells were left to recover overnight after sorting, and then treated with 0.5 mg/ml bevacizumab for 4 d, with SU1498 (5 µM) for 24 h, or vehicle-treated and then injected into striatum of BALB/c (nu/nu) mice.

Immunoblot analysis and immunoprecipitation. Whole-cell extracts or immunoprecipitated complexes of VEGFR2 were separated by 7% SDS-PAGE and transferred to nitrocellulose membranes (Advantech) using the iBlot System (Invitrogen). The membranes were blocked with 5% (wt/vol) dry milk in PBS-Tween-20 (0.5% vol/vol) and probed with primary antibodies against total VEGFR2 (Cell Signaling Technology; 1:2,000), phosphorylated VEGFR2 (VEGFR2Tyr1054; 1:200; Millipore), NRP1 (Abcam; 1:500), NRP1 (Santa Cruz Biotechnology, Inc.; 1:500), EEA1 (Abcam; 1:300), ERK1/2 (Cell Signaling Technology; 1:800), or against α-tubulin (Sigma-Aldrich) as a loading control. ECL detection system was used according to manufacturer's instructions (GE Healthcare).

Biotinylation/recycling assay and membrane protein isolation. To measure the relative proportions of the surface and internalized VEGFR2 pools, cell surface protein biotin-labeling using a Cell Surface Protein Isolation kit (Thermo Fisher Scientific) was used according to the manufacturer's instructions. Equal volumes (30 µl) from cytosolic and membrane fractions were loaded onto a 7% SDS-PAGE gel and probed for the presence of VEGFR2, and ERK1/2 detection was used as a purity control of the cytosolic or membrane fractions. Receptor recycling assay using biotinylation and biotin reduction (stripping) steps was performed as previously described (Jopling et al., 2011). Here, cells were washed twice in PBS, resuspended in a cleavable NHS-SS-Biotin solution (0.3 mg/ml; +Bio) or Biotin-free solution (for negative control; −BIO), and incubated for 30 min on ice. Control samples (−Bio; +Bio) were then quenched and lysed. For a strip control (Strip), cells were exposed to a reducing buffer (100 mM sodium 2-mercapthoethanolsufonate, 50 mM Tris, pH 8.6, 100 mM sodium chloride, 1 mM EDTA, and 0.2% [wt/vol] BSA) to cleave the biotin label.

To obtain other samples (Inter, to search for internalized receptor; Recy, to detect a potentially recycled/resurfaced receptor), cells were biotin-labeled and incubated in GF-free medium for 10 min at 37°C. After incubation, cell-surface biotin was removed using a reducing buffer and quenched in a buffer containing 120 mM iodoacetamide. The cell sample used to search for internalized receptor (Inter; where the originally cell surface-biotinylated VEGFR2 has internalized into cytosol, and thus was protected from the reducing/stripping treatment responsible for biotin cleavage) was subjected to lysis and immunoprecipitation. The cells for detection of recycled receptor (Recy and Recy-con) were incubated for another 20 min in growth factor–free medium at 37°C, followed by the reduction step (Recy sample only, to allow for potential recycling of the receptor back to cell surface, where it became susceptible to the biotin strip using the reduction buffer), before lysis and immunoprecipitation. Recy-con served as a control for potential degradation of biotinylated VEGFR2, processed along with the Recy sample, except that the last reduction step was omitted to detect total levels of biotinylated receptor remaining at that time. The entire immunoprecipitated protein amount was used in each case for loading SDS-PAGE for immunoblotting analysis of VEGFR2, NRP1, and TfR as described above.

FACS analysis of surface and total VEGFR2. FACS analysis of surface versus total VEGFR2 was performed as described previously (Ostrowski et al., 2010), for Fig. 1 D with minor modification of using a primary conjugated anti-VEGFR2 antibody (Alexa Fluor 488; BioLegend) for the first labeling step and an unconjugated primary anti-VEGFR2 antibody (followed by a secondary Alexa Fluor 647–conjugated antibody) for the second labeling step. For other experiments, the freshly dissociated GBM cells were left to recover overnight, and then surface VEGFR2 labeling of living cells (using a monoclonal rabbit anti-VEGFR2 antibody, followed by a secondary anti–rabbit antibody conjugated to Alexa Fluor 488) on ice was performed.

Next, although one part of such surface-labeled cells could be analyzed by FACS, the remaining cells after surface labeling were fixed and permeabilized with 0.2% Triton X-100 in PBS, and the second round of labeling using the same primary and secondary antibody was used, thereby visualizing total cellular VEGFR2. Each labeling step was followed by three acidic wash steps to remove any unbound antibodies.

Lentiviral shRNA particle preparation and cell transduction. Lentiviral shRNA particles (The RNAi Consortium shRNA collection; Sigma-Aldrich) were prepared according to published procedures (Stewart et al., 2003; Moffat et al., 2006; Tiscornia et al., 2006). Viral titer was estimated by ELISA p24 (Takara Bio Inc.) and equal titers were used for infection of VEGFR2-sorted cells. 2 d after infection, cells were selected with puromycin for 48 h, and then used for evaluation of apoptosis, cell viability, and in vivo tumor formation.

Growth curves/proliferation and caspase 3/7 assay. Cells were plated into a 96-well plate at 3,000 cells per well in triplicate immediately after treatments. Cell viability was measured in growth factor free media for up to 7 d using the CellTiter-Glo assay kit (Promega). The caspase 3/7 activity was measured using the Caspase-Glo 3/7 assay (Promega) according to the manufacturer's instructions.

VEGF ELISA. $VEGFR2^{H}$ and $VEGFR2^{L}$ cells were left to recover overnight, and then left untreated or treated for 24 h in growth factor–free medium. As indicated at 24 h after treatment (5 μM SU1498, 0.5 mg/ml bevacizumab, or left untreated), cell suspension was spun down at 2,000 rpm and supernatant was analyzed by ELISA. 200 μl of conditioned media were collected from triplicate samples. Human VEGF Quantikine ELISA kit (R&D Systems) was used according to the directions of the manufacturer.

In vivo tumor formation. In vivo tumor formation was performed as described previously (Bao et al., 2006a; Lathia et al., 2010). For studies involving comparison of $VEGFR2^{H}$ versus $VEGFR2^{L}$ cells, 100, 1,000, 5,000, or 10,000 cells were transplanted into striatum of BALB/c (nu/nu) mice (4–6 per group) after 2 h of recovery after FACS sorting under a Cleveland Clinic Foundation Institutional Animal Care and Use Committee–approved protocol. For VEGFR2 shRNA studies, 10,000 viable puromycin-selected cells were injected as described above.

Statistical analysis. Values are reported as the mean ± SD. GraphPad Prism Software (GraphPad Software, Inc.) was used to examine statistical significance with Student's *t* test, by log-rank, or one-way ANOVA.

Online supplemental material. Fig. S1 shows FACS analysis of CD31, CD34, CD105, and CD144 endothelial markers in $VEGFR2^{H}$ GBM cells. Table S1 shows tumor incidence and median survival. Online supplemental material is available at http://www.jem.org/cgi/content/full/jem.20111424/DC1.

This work was supported by grants from the following organizations: the Danish Council for Independent Research/Medical Sciences ID4765/11-105457 (P. Hamerlik); Czech Ministry of Education (MSM6198959216); Czech Ministry of Health (NT11065-5); European Commission (projects Infla-Care, CZ.1.07/2.3.00/20.0019, CZ.1.05/2.1.00/01.0030, Trireme, DDResponse); the Danish National Research Foundation; the National Institutes of Health (grants NS054276, CA129958, CA116659, and CA154130 [all to J.N. Rich]); and a National Research Service Award CA142159 (J.D. Lathia). J.N. Rich is a Damon Runyon-Lilly Clinical Investigator supported by the Damon Runyon Cancer Research Foundation. J.D. Lathia is supported by an American Brain Tumor Association Fellowship (sponsored by the Joelle Syverson Fund).

The authors have no conflicting financial interests.

Submitted: 12 July 2011
Accepted: 7 February 2012

REFERENCES

Ballmer-Hofer, K., A.E. Andersson, L.E. Ratcliffe, and P. Berger. 2011. Neuropilin-1 promotes VEGFR-2 trafficking through Rab11 vesicles thereby specifying signal output. *Blood*. 118:816–826. http://dx.doi.org/10.1182/blood-2011-01-328773

Bao, S., Q. Wu, R.E. McLendon, Y. Hao, Q. Shi, A.B. Hjelmeland, M.W. Dewhirst, D.D. Bigner, and J.N. Rich. 2006a. Glioma stem cells promote radioresistance by preferential activation of the DNA damage response. *Nature*. 444:756–760. http://dx.doi.org/10.1038/nature05236

Bao, S., Q. Wu, S. Sathornsumetee, Y. Hao, Z. Li, A.B. Hjelmeland, Q. Shi, R.E. McLendon, D.D. Bigner, and J.N. Rich. 2006b. Stem cell-like glioma cells promote tumor angiogenesis through vascular endothelial growth factor. *Cancer Res*. 66:7843–7848. http://dx.doi.org/10.1158/0008-5472.CAN-06-1010

Bartkova, J., Z. Horejsí, K. Koed, A. Krämer, F. Tort, K. Zieger, P. Guldberg, M. Sehested, J.M. Nesland, C. Lukas, T. Ørntoft, J. Lukas, and J. Bartek. 2005. DNA damage response as a candidate anti-cancer barrier in early human tumorigenesis. *Nature*. 434:864–870. httpx://dx.doi.org/10.1038/nature03482

Beier, D., P. Hau, M. Proescholdt, A. Lohmeier, J. Wischhusen, P.J. Oefner, L. Aigner, A. Brawanski, U. Bogdahn, and C.P. Beier. 2007. CD133(+) and CD133(-) glioblastoma-derived cancer stem cells show differential growth characteristics and molecular profiles. *Cancer Res*. 67:4010–4015. http://dx.doi.org/10.1158/0008-5472.CAN-06-4180

Butler, J.M., H. Kobayashi, and S. Rafii. 2010. Instructive role of the vascular niche in promoting tumour growth and tissue repair by angiocrine factors. *Nat. Rev. Cancer*. 10:138–146. http://dx.doi.org/10.1038/nrc2791

Calabrese, C., H. Poppleton, M. Kocak, T.L. Hogg, C. Fuller, B. Hamner, E.Y. Oh, M.W. Gaber, D. Finklestein, M. Allen, et al. 2007. A perivascular niche for brain tumor stem cells. *Cancer Cell*. 11:69–82. http://dx.doi.org/10.1016/j.ccr.2006.11.020

Christensen, K., H.D. Schrøder, and B.W. Kristensen. 2011. CD133+ niches and single cells in glioblastoma have different phenotypes. *J. Neurooncol*. 104:129–143. http://dx.doi.org/10.1007/s11060-010-0488-y

Citrin, D., C. Ménard, and K. Camphausen. 2006. Combining radiotherapy and angiogenesis inhibitors: clinical trial design. *Int. J. Radiat. Oncol. Biol. Phys*. 64:15–25. http://dx.doi.org/10.1016/j.ijrobp.2005.03.065

Desjardins, A., D.A. Reardon, J.E. Herndon II, J. Marcello, J.A. Quinn, J.N. Rich, S. Sathornsumetee, S. Gururangan, J. Sampson, L. Bailey, et al. 2008. Bevacizumab plus irinotecan in recurrent WHO grade 3 malignant gliomas. *Clin. Cancer Res*. 14:7068–7073. http://dx.doi.org/10.1158/1078-0432.CCR-08-0260

Ellis, L.M., and D.J. Hicklin. 2008. VEGF-targeted therapy: mechanisms of anti-tumour activity. *Nat. Rev. Cancer*. 8:579–591. http://dx.doi.org/10.1038/nrc2403

Eyler, C.E., and J.N. Rich. 2008. Survival of the fittest: cancer stem cells in therapeutic resistance and angiogenesis. *J. Clin. Oncol*. 26:2839–2845. http://dx.doi.org/10.1200/JCO.2007.15.1829

Eyler, C.E., W.C. Foo, K.M. LaFiura, R.E. McLendon, A.B. Hjelmeland, and J.N. Rich. 2008. Brain cancer stem cells display preferential sensitivity to Akt inhibition. *Stem Cells*. 26:3027–3036. http://dx.doi.org/10.1634/stemcells.2007-1073

Ferrara, N., H.P. Gerber, and J. LeCouter. 2003. The biology of VEGF and its receptors. *Nat. Med*. 9:669–676. http://dx.doi.org/10.1038/nm0603-669

Folkins, C., S. Man, P. Xu, Y. Shaked, D.J. Hicklin, and R.S. Kerbel. 2007. Anticancer therapies combining antiangiogenic and tumor cell cytotoxic effects reduce the tumor stem-like cell fraction in glioma xenograft tumors. *Cancer Res*. 67:3560–3564. http://dx.doi.org/10.1158/0008-5472.CAN-06-4238

Folkins, C., Y. Shaked, S. Man, T. Tang, C.R. Lee, Z. Zhu, R.M. Hoffman, and R.S. Kerbel. 2009. Glioma tumor stem-like cells promote tumor angiogenesis and vasculogenesis via vascular endothelial growth factor and stromal-derived factor 1. *Cancer Res*. 69:7243–7251. http://dx.doi.org/10.1158/0008-5472.CAN-09-0167

Friedman, H.S., M.D. Prados, P.Y. Wen, T. Mikkelsen, D. Schiff, L.E. Abrey, W.K. Yung, N. Paleologos, M.K. Nicholas, R. Jensen, et al.

2009. Bevacizumab alone and in combination with irinotecan in recurrent glioblastoma. *J. Clin. Oncol.* 27:4733–4740. http://dx.doi.org/10.1200/JCO.2008.19.8721

Gampel, A., L. Moss, M.C. Jones, V. Brunton, J.C. Norman, and H. Mellor. 2006. VEGF regulates the mobilization of VEGFR2/KDR from an intracellular endothelial storage compartment. *Blood.* 108:2624–2631. http://dx.doi.org/10.1182/blood-2005-12-007484

Gilbertson, R.J., and J.N. Rich. 2007. Making a tumour's bed: glioblastoma stem cells and the vascular niche. *Nat. Rev. Cancer.* 7:733–736. http://dx.doi.org/10.1038/nrc2246

Gorski, D.H., M.A. Beckett, N.T. Jaskowiak, D.P. Calvin, H.J. Mauceri, R.M. Salloum, S. Seetharam, A. Koons, D.M. Hari, D.W. Kufe, and R.R. Weichselbaum. 1999. Blockage of the vascular endothelial growth factor stress response increases the antitumor effects of ionizing radiation. *Cancer Res.* 59:3374–3378.

Graeven, U., W. Fiedler, S. Karpinski, S. Ergün, N. Kilic, U. Rodeck, W. Schmiegel, and D.K. Hossfeld. 1999. Melanoma-associated expression of vascular endothelial growth factor and its receptors FLT-1 and KDR. *J. Cancer Res. Clin. Oncol.* 125:621–629. http://dx.doi.org/10.1007/s004320050325

Gururangan, S., S.N. Chi, T. Young Poussaint, A. Onar-Thomas, R.J. Gilbertson, S. Vajapeyam, H.S. Friedman, R.J. Packer, B.N. Rood, J.M. Boyett, and L.E. Kun. 2010. Lack of efficacy of bevacizumab plus irinotecan in children with recurrent malignant glioma and diffuse brainstem glioma: a Pediatric Brain Tumor Consortium study. *J. Clin. Oncol.* 28:3069–3075. http://dx.doi.org/10.1200/JCO.2009.26.8789

Hemmati, H.D., I. Nakano, J.A. Lazareff, M. Masterman-Smith, D.H. Geschwind, M. Bronner-Fraser, and H.I. Kornblum. 2003. Cancerous stem cells can arise from pediatric brain tumors. *Proc. Natl. Acad. Sci. USA.* 100:15178–15183. http://dx.doi.org/10.1073/pnas.2036535100

Hess, C., V. Vuong, I. Hegyi, O. Riesterer, J. Wood, D. Fabbro, C. Glanzmann, S. Bodis, and M. Pruschy. 2001. Effect of VEGF receptor inhibitor PTK787/ZK222584 [correction of ZK222548] combined with ionizing radiation on endothelial cells and tumour growth. *Br. J. Cancer.* 85:2010–2016. http://dx.doi.org/10.1054/bjoc.2001.2166

Hlobilkova, A., J. Ehrmann, P. Knizetova, V. Krejci, O. Kalita, and Z. Kolar. 2009. Analysis of VEGF, Flt-1, Flk-1, nestin and MMP-9 in relation to astrocytoma pathogenesis and progression. *Neoplasma.* 56:284–290. http://dx.doi.org/10.4149/neo_2009_04_284

Hu, B., P. Guo, I. Bar-Joseph, Y. Imanishi, M.J. Jarzynka, O. Bogler, T. Mikkelsen, T. Hirose, R. Nishikawa, and S.Y. Cheng. 2007. Neuropilin-1 promotes human glioma progression through potentiating the activity of the HGF/SF autocrine pathway. *Oncogene.* 26:5577–5586. http://dx.doi.org/10.1038/sj.onc.1210348

Ishida, S., K. Shinoda, S. Kawashima, Y. Oguchi, Y. Okada, and E. Ikeda. 2000. Coexpression of VEGF receptors VEGF-R2 and neuropilin-1 in proliferative diabetic retinopathy. *Invest. Ophthalmol. Vis. Sci.* 41: 1649–1656.

Iwamoto, F.M., and H.A. Fine. 2010. Bevacizumab for malignant gliomas. *Arch. Neurol.* 67:285–288. http://dx.doi.org/10.1001/archneurol.2010.11

Iwamoto, F.M., L.E. Abrey, K. Beal, P.H. Gutin, M.K. Rosenblum, V.E. Reuter, L.M. DeAngelis, and A.B. Lassman. 2009. Patterns of relapse and prognosis after bevacizumab failure in recurrent glioblastoma. *Neurology.* 73:1200–1206. http://dx.doi.org/10.1212/WNL.0b013e3181bc0184

Jarvis, A., C.K. Allerston, H. Jia, B. Herzog, A. Garza-Garcia, N. Winfield, K. Ellard, R. Aqil, R. Lynch, C. Chapman, et al. 2010. Small molecule inhibitors of the neuropilin-1 vascular endothelial growth factor A (VEGF-A) interaction. *J. Med. Chem.* 53:2215–2226. http://dx.doi.org/10.1021/jm901755g

Joo, K.M., S.Y. Kim, X. Jin, S.Y. Song, D.S. Kong, J.I. Lee, J.W. Jeon, M.H. Kim, B.G. Kang, Y. Jung, et al. 2008. Clinical and biological implications of CD133-positive and CD133-negative cells in glioblastomas. *Lab. Invest.* 88:808–815. http://dx.doi.org/10.1038/labinvest.2008.57

Jopling, H.M., G.J. Howell, N. Gamper, and S. Ponnambalam. 2011. The VEGFR2 receptor tyrosine kinase undergoes constitutive endosome-to-plasma membrane recycling. *Biochem. Biophys. Res. Commun.* 410:170–176. http://dx.doi.org/10.1016/j.bbrc.2011.04.093

Knizetova, P., J. Ehrmann, A. Hlobilkova, I. Vancova, O. Kalita, Z. Kolar, and J. Bartek. 2008. Autocrine regulation of glioblastoma cell cycle progression, viability and radioresistance through the VEGF-VEGFR2 (KDR) interplay. *Cell Cycle.* 7:2553–2561. http://dx.doi.org/10.4161/cc.7.16.6442

Kremer, C., G. Breier, W. Risau, and K.H. Plate. 1997. Up-regulation of flk-1/vascular endothelial growth factor receptor 2 by its ligand in a cerebral slice culture system. *Cancer Res.* 57:3852–3859.

Lai, A., A. Tran, P.L. Nghiemphu, W.B. Pope, O.E. Solis, M. Selch, E. Filka, W.H. Yong, P.S. Mischel, L.M. Liau, et al. 2011. Phase II study of bevacizumab plus temozolomide during and after radiation therapy for patients with newly diagnosed glioblastoma multiforme. *J. Clin. Oncol.* 29:142–148. http://dx.doi.org/10.1200/JCO.2010.30.2729

Lampugnani, M.G., F. Orsenigo, M.C. Gagliani, C. Tacchetti, and E. Dejana. 2006. Vascular endothelial cadherin controls VEGFR-2 internalization and signaling from intracellular compartments. *J. Cell Biol.* 174:593–604. http://dx.doi.org/10.1083/jcb.200602080

Lathia, J.D., J. Gallagher, J.M. Heddleston, J. Wang, C.E. Eyler, J. Macswords, Q. Wu, A. Vasanji, R.E. McLendon, A.B. Hjelmeland, and J.N. Rich. 2010. Integrin alpha 6 regulates glioblastoma stem cells. *Cell Stem Cell.* 6:421–432. http://dx.doi.org/10.1016/j.stem.2010.02.018

Leone, D.P., J.B. Relvas, L.S. Campos, S. Hemmi, C. Brakebusch, R. Fässler, C. Ffrench-Constant, and U. Suter. 2005. Regulation of neural progenitor proliferation and survival by beta1 integrins. *J. Cell Sci.* 118:2589–2599. http://dx.doi.org/10.1242/jcs.02396

Li, Z., S. Bao, Q. Wu, H. Wang, C. Eyler, S. Sathornsumetee, Q. Shi, Y. Cao, J. Lathia, R.E. McLendon, et al. 2009a. Hypoxia-inducible factors regulate tumorigenic capacity of glioma stem cells. *Cancer Cell.* 15:501–513. http://dx.doi.org/10.1016/j.ccr.2009.03.018

Li, Z., H. Wang, C.E. Eyler, A.B. Hjelmeland, and J.N. Rich. 2009b. Turning cancer stem cells inside out: an exploration of glioma stem cell signaling pathways. *J. Biol. Chem.* 284:16705–16709. http://dx.doi.org/10.1074/jbc.R900013200

Liu, G., X. Yuan, Z. Zeng, P. Tunici, H. Ng, I.R. Abdulkadir, L. Lu, D. Irvin, K.L. Black, and J.S. Yu. 2006. Analysis of gene expression and chemoresistance of CD133+ cancer stem cells in glioblastoma. *Mol. Cancer.* 5:67. http://dx.doi.org/10.1186/1476-4598-5-67

Mac Gabhann, F., and A.S. Popel. 2006. Targeting neuropilin-1 to inhibit VEGF signaling in cancer: Comparison of therapeutic approaches. *PLOS Comput. Biol.* 2:e180. http://dx.doi.org/10.1371/journal.pcbi.0020180

Meissner, M., G. Reichenbach, M. Stein, I. Hrgovic, R. Kaufmann, and J. Gille. 2009. Down-regulation of vascular endothelial growth factor receptor 2 is a major molecular determinant of proteasome inhibitor-mediated antiangiogenic action in endothelial cells. *Cancer Res.* 69:1976–1984. http://dx.doi.org/10.1158/0008-5472.CAN-08-3150

Moffat, J., D.A. Grueneberg, X. Yang, S.Y. Kim, A.M. Kloepfer, G. Hinkle, B. Piqani, T.M. Eisenhaure, B. Luo, J.K. Grenier, et al. 2006. A lentiviral RNAi library for human and mouse genes applied to an arrayed viral high-content screen. *Cell.* 124:1283–1298. http://dx.doi.org/10.1016/j.cell.2006.01.040

Newman, P.J., M.C. Berndt, J. Gorski, G.C. White II, S. Lyman, C. Paddock, and W.A. Muller. 1990. PECAM-1 (CD31) cloning and relation to adhesion molecules of the immunoglobulin gene superfamily. *Science.* 247:1219–1222. http://dx.doi.org/10.1126/science.1690453

Norden, A.D., and P.Y. Wen. 2006. Glioma therapy in adults. *Neurologist.* 12:279–292. http://dx.doi.org/10.1097/01.nrl.0000250928.26044.47

Norden, A.D., J. Drappatz, and P.Y. Wen. 2009. Antiangiogenic therapies for high-grade glioma. *Nat. Rev. Neurol.* 5:610–620. http://dx.doi.org/10.1038/nrneurol.2009.159

Ogden, A.T., A.E. Waziri, R.A. Lochhead, D. Fusco, K. Lopez, J.A. Ellis, J. Kang, M. Assanah, G.M. McKhann, M.B. Sisti, et al. 2008. Identification of A2B5+CD133- tumor-initiating cells in adult human gliomas. *Neurosurgery.* 62:505–514. http://dx.doi.org/10.1227/01.neu.0000316019.28421.95

Ostrowski, M., N.B. Carmo, S. Krumeich, I. Fanget, G. Raposo, A. Savina, C.F. Moita, K. Schauer, A.N. Hume, R.P. Freitas, et al. 2010. Rab27a and Rab27b control different steps of the exosome secretion pathway. *Nat. Cell Biol.* 12:19–30.

Pan, Q., Y. Chanthery, W.C. Liang, S. Stawicki, J. Mak, N. Rathore, R.K. Tong, J. Kowalski, S.F. Yee, G. Pacheco, et al. 2007. Blocking neuropilin-1 function has an additive effect with anti-VEGF to inhibit tumor growth. *Cancer Cell*. 11:53–67. http://dx.doi.org/10.1016/j.ccr.2006.10.018

Reya, T., S.J. Morrison, M.F. Clarke, and I.L. Weissman. 2001. Stem cells, cancer, and cancer stem cells. *Nature*. 414:105–111. http://dx.doi.org/10.1038/35102167

Ricci-Vitiani, L., R. Pallini, M. Biffoni, M. Todaro, G. Invernici, T. Cenci, G. Maira, E.A. Parati, G. Stassi, L.M. Larocca, and R. De Maria. 2010. Tumour vascularization via endothelial differentiation of glioblastoma stem-like cells. *Nature*. 468:824–828. http://dx.doi.org/10.1038/nature09557

Rich, J.N. 2007. Cancer stem cells in radiation resistance. *Cancer Res*. 67:8980–8984. http://dx.doi.org/10.1158/0008-5472.CAN-07-0895

Roberts, M., S. Barry, A. Woods, P. van der Sluijs, and J. Norman. 2001. PDGF-regulated rab4-dependent recycling of alphavbeta3 integrin from early endosomes is necessary for cell adhesion and spreading. *Curr. Biol.* 11:1392–1402. http://dx.doi.org/10.1016/S0960-9822(01)00442-0

Rosenstein, J.M., and J.M. Krum. 2004. New roles for VEGF in nervous tissue—beyond blood vessels. *Exp. Neurol*. 187:246–253. http://dx.doi.org/10.1016/j.expneurol.2004.01.022

Sakariassen, P.O., L. Prestegarden, J. Wang, K.O. Skaftnesmo, R. Mahesparan, C. Molthoff, P. Sminia, E. Sundlisaeter, A. Misra, B.B. Tysnes, et al. 2006. Angiogenesis-independent tumor growth mediated by stem-like cancer cells. *Proc. Natl. Acad. Sci. USA*. 103:16466–16471. http://dx.doi.org/10.1073/pnas.0607668103

Shen, R., Y. Ye, L. Chen, Q. Yan, S.H. Barsky, and J.X. Gao. 2008. Precancerous stem cells can serve as tumor vasculogenic progenitors. *PLoS ONE*. 3:e1652. http://dx.doi.org/10.1371/journal.pone.0001652

Shibuya, M. 2008. Vascular endothelial growth factor-dependent and -independent regulation of angiogenesis. *BMB Rep*. 41:278–286. http://dx.doi.org/10.5483/BMBRep.2008.41.4.278

Shintani, S., C. Li, M. Mihara, S.K. Klosek, N. Terakado, S. Hino, and H. Hamakawa. 2006. Anti-tumor effect of radiation response by combined treatment with angiogenesis inhibitor, TNP-470, in oral squamous cell carcinoma. *Oral Oncol*. 42:66–72. http://dx.doi.org/10.1016/j.oraloncology.2005.06.010

Singh, S.K., I.D. Clarke, M. Terasaki, V.E. Bonn, C. Hawkins, J. Squire, and P.B. Dirks. 2003. Identification of a cancer stem cell in human brain tumors. *Cancer Res*. 63:5821–5828.

Soda, Y., T. Marumoto, D. Friedmann-Morvinski, M. Soda, F. Liu, H. Michiue, S. Pastorino, M. Yang, R.M. Hoffman, S. Kesari, and I.M. Verma. 2011. Transdifferentiation of glioblastoma cells into vascular endothelial cells. *Proc. Natl. Acad. Sci. USA*. 108:4274–4280. http://dx.doi.org/10.1073/pnas.1016030108

Soker, S., H.Q. Miao, M. Nomi, S. Takashima, and M. Klagsbrun. 2002. VEGF165 mediates formation of complexes containing VEGFR-2 and neuropilin-1 that enhance VEGF165-receptor binding. *J. Cell. Biochem*. 85:357–368. http://dx.doi.org/10.1002/jcb.10140

Son, M.J., K. Woolard, D.H. Nam, J. Lee, and H.A. Fine. 2009. SSEA-1 is an enrichment marker for tumor-initiating cells in human glioblastoma. *Cell Stem Cell*. 4:440–452. http://dx.doi.org/10.1016/j.stem.2009.03.003

Stewart, S.A., D.M. Dykxhoorn, D. Palliser, H. Mizuno, E.Y. Yu, D.S. An, D.M. Sabatini, I.S. Chen, W.C. Hahn, P.A. Sharp, et al. 2003. Lentivirus-delivered stable gene silencing by RNAi in primary cells. *RNA*. 9:493–501. http://dx.doi.org/10.1261/rna.2192803

Tiscornia, G., O. Singer, and I.M. Verma. 2006. Production and purification of lentiviral vectors. *Nat. Protoc*. 1:241–245. http://dx.doi.org/10.1038/nprot.2006.37

Tokuyama, W., T. Mikami, M. Masuzawa, and I. Okayasu. 2010. Autocrine and paracrine roles of VEGF/VEGFR-2 and VEGF-C/VEGFR-3 signaling in angiosarcomas of the scalp and face. *Hum. Pathol*. 41:407–414. http://dx.doi.org/10.1016/j.humpath.2009.08.021

Verhoeff, J.J., O. van Tellingen, A. Claes, L.J. Stalpers, M.E. van Linde, D.J. Richel, W.P. Leenders, and W.R. van Furth. 2009. Concerns about anti-angiogenic treatment in patients with glioblastoma multiforme. *BMC Cancer*. 9:444. http://dx.doi.org/10.1186/1471-2407-9-444

Verhoeff, J.J., C. Lavini, M.E. van Linde, L.J. Stalpers, C.B. Majoie, J.C. Reijneveld, W.R. van Furth, and D.J. Richel. 2010. Bevacizumab and dose-intense temozolomide in recurrent high-grade glioma. *Ann. Oncol*. 21:1723–1727. http://dx.doi.org/10.1093/annonc/mdp591

Vredenburgh, J.J., A. Desjardins, J.E. Herndon II, J. Marcello, D.A. Reardon, J.A. Quinn, J.N. Rich, S. Sathornsumetee, S. Gururangan, J. Sampson, et al. 2007. Bevacizumab plus irinotecan in recurrent glioblastoma multiforme. *J. Clin. Oncol*. 25:4722–4729. http://dx.doi.org/10.1200/JCO.2007.12.2440

Wang, J., P.O. Sakariassen, O. Tsinkalovsky, H. Immervoll, S.O. Bøe, A. Svendsen, L. Prestegarden, G. Røsland, F. Thorsen, L. Stuhr, et al. 2008. CD133 negative glioma cells form tumors in nude rats and give rise to CD133 positive cells. *Int. J. Cancer*. 122:761–768. http://dx.doi.org/10.1002/ijc.23130

Wang, R., K. Chadalavada, J. Wilshire, U. Kowalik, K.E. Hovinga, A. Geber, B. Fligelman, M. Leversha, C. Brennan, and V. Tabar. 2010. Glioblastoma stem-like cells give rise to tumour endothelium. *Nature*. 468:829–833. http://dx.doi.org/10.1038/nature09624

Wherlock, M., A. Gampel, C. Futter, and H. Mellor. 2004. Farnesyltransferase inhibitors disrupt EGF receptor traffic through modulation of the RhoB GTPase. *J. Cell Sci*. 117:3221–3231. http://dx.doi.org/10.1242/jcs.01193

Winkler, F., S.V. Kozin, R.T. Tong, S.S. Chae, M.F. Booth, I. Garkavtsev, L. Xu, D.J. Hicklin, D. Fukumura, E. di Tomaso, et al. 2004. Kinetics of vascular normalization by VEGFR2 blockade governs brain tumor response to radiation: role of oxygenation, angiopoietin-1, and matrix metalloproteinases. *Cancer Cell*. 6:553–563.

Wu, Y., and P.Y. Wu. 2009. CD133 as a marker for cancer stem cells: progresses and concerns. *Stem Cells Dev*. 18:1127–1134. http://dx.doi.org/10.1089/scd.2008.0338

Xiao, Z., Y. Kong, S. Yang, M. Li, J. Wen, and L. Li. 2007. Upregulation of Flk-1 by bFGF via the ERK pathway is essential for VEGF-mediated promotion of neural stem cell proliferation. *Cell Res*. 17:73–79. http://dx.doi.org/10.1038/sj.cr.7310126